Applied problems of nonlinear oscillation and wave theory

Izv. VUZ. «AND», vol. 11, № 3, 2003

NOISY NEURAL RHYTHM GENERATORS

E. Mosekilde, O.V. Sosnovtseva, D. Postnov, H.A. Braun, and M.T. Huber

The dynamical features of spike train generation in the presence of noise are investigated for three different models of neural rhythm generators: a single neuron model that simulates impulse pattern modulation for temperature encoding in mammalian cold receptors, a minimal neural network that describes transitions between beta and gamma rhythms in the brain and an electronic switching device that represents a simple breathing rhythm generator for a snail. We show that noise can explain a number of peculiarities in the observed spike trains, cause coherent switchings between different states, and induce new rhythms in small neural ensembles.

1. Introduction

Noise can introduce multivarious effects especially in nonlinear and chaotic systems and makes the dynamics of such systems still more difficult to understand. Vadim S. Anishchenko, together with his group, has made major contributions towards a better understanding of nonlinear and chaotic systems under the influence of noise [1,2]. Such approaches can become of particular value for the understanding of pattern generation in neuronal systems because neurons are inherently nonlinear, often chaotic and inevitably contaminated with noise.

The spatiotemporal characteristics of neural firing patterns in connection with brain function have received considerable interest, and many studies have been performed in order to understand the origin and role of various forms of synchronized neural activity (e.g., [3,4]). Even single functional units demonstrate flexible neuronal patterns, and experimental recordings of peripheral sensory receptors and central neurons show more or less continuous transitions between different types of oscillatory patterns as a function of physiologically relevant stimuli [5,6]. In accordance with experimental observations on mammalian cold receptors, the Huber/Braun model [7], for example, reproduces tonic activities or bursting discharges due to slow oscillation cycles each triggering a group of impulses during its suprathreshold phase. Moreover, there exist irregular patterns of apparently chaotic origin [8,9] while other patterns that can be explained only with essential contributions of noise are typical for thermosensitive neurons [6].

The complex and multifarious effects of noise on neural firing have not yet been fully understood. Neural activity is known to be noisy [10], and this stochastic feature is observed during both information transmission and spontaneous firing. At the same time, noise can play a constructive role in neural systems. In the presence of a subthreshold signal, the excitation threshold may be crossed when noise is superimposed onto the

signal. This happens with high probability when the signal has its maximum and, hence, allows the biological system to detect signals that without noise would remain subthreshold [11,12], demonstrating the effect of stochastic resonance [13]. An excitable neuronal system can exhibit the related phenomenon of coherence resonance [14]. In this case, there is no underlying periodic signal, and the resonance phenomenon is controlled by the noise intensity and the time of relaxation. Stochastic synchronization phenomena, i.e., the synchronization of noise-activated or noise-induced rhythms, have been studied in electrosensitive cells of the paddlefish by Neiman *et al.* [15]. Different types of noisy phase-locked regimes were observed.

Many neural systems can perform oscillations in different modes. Hence, the interesting questions arise: How is the dynamics of neural firing with *multimode* behavior affected by noise, and under what conditions can noise activate new rhythms? In this paper we focus on the following aspects:

(i) how can the presence of noise interfere with the spike generating mechanisms and the subthreshold oscillations in peripheral pattern generators, and under what conditions can it completely change the spiking pattern? The intrinsic dynamics is characterized by oscillatory changes in the membrane potential that are below or close to the spike threshold. In this situation naturally occurring stochastic influences due to membrane or synaptic noise can be an essential component in signal encoding. The reason is that the noise actually determines whether a spike is triggered during an oscillatory cycle or not. Hence, mixed patterns typically result, consisting of random sequences of spike-triggering and subthreshold oscillations;

(ii) how is the switching process between coexisting rhythmic activities in the brain influenced by noise? Brain oscillations are normally divided into different types based mainly on their frequency. Rhythms in the β (12-30 Hz) and the γ (30-80 Hz) ranges are found in many parts of the nervous system and are associated with attention, perception and cognition. Recently Kopell *et al.* [16] demonstrated that a model including both inhibitory interneurons and excitatory pyramidal cells can produce β as well as γ oscillations that employ different dynamical mechanisms to synchronize. The β mode is able to synchronize with long conduction delays corresponding to signals traveling over a significant distance in the brain. Similar distances can not be tolerated by the γ rhythms that are used more for local communication. It has been noted in electroencephalogram signals that rhythms of different frequencies can be found simultaneously [17]. In this connection we describe noise-induced activities in terms of regularized switching events;

(iii) how can noise control the appearance of additional time scales in small neuron ensembles? In contrast to previous studies we investigate *noise-induced* rather than noise-activated oscillatory modes, i.e., we focus on time scales that are produced and controlled by noise and that do not exist in the deterministic case. We provide experimental observation of such multimode behavior and investigate the conditions for generation and entrainment of the various modes.

2. Tuning cold-receptor discharges

2.1. The Huber/Braun model. Mammalian cold receptors are particularly interesting in connection with the present analysis, both because of the complicated impulse patterns that they generate and because of the clear influence of noise. The impulse patterns are generally characterized by regular and relatively frequent burst discharges at intermediate temperatures with irregular and less frequent bursting patterns occurring at lower temperatures and irregular single spike discharges observed at higher temperatures. The stationary frequency *vs* temperature characteristic typically displays a maximum at intermediate temperatures (25-30°C). This lack of monotonicity implies that

the temperature encoding must be associated with the firing pattern as such and not only with the average firing rate. The Huber/Braun model of mammalian cold receptor was described in detail in Refs [7,18]. In brief, it consists of two interacting minimal sets of ionic conductances, each including simplified de- and repolarizing Hodgkin-Huxley-type currents with sigmoidal steady state activation kinetics. For simplicity, inactivation is neglected. The two sets operate at different voltage levels and time scales. High threshold, fast activating currents are for spike generation (marked by indices *d* and *r*); low threshold, slow activating currents generate subthreshold potential oscillations (indices *sd* and *sr*). Including a leakage current I_l and the applied current I_{appl}, the membrane potential V is given by:

$$c\dot{V} = -I_l - I_d - I_r - I_{sd} - I_{sr} - I_{appl}, \tag{1}$$

with c denoting the membrane capacitance. In our generalized approach we do not refer to specific ionic currents but to the de- and repolarizing components of the two subsystems, the spike generator and the subthreshold oscillator. I_d is the fast depolarizing current and I_r is the fast repolarizing current which reflect the classical Na^+- and K^+-currents in the spike generation. The physiological basis for the two other currents, I_{sd} and I_{sr}, may be different in different neurons.

The leakage current is given by

$$I_l = g_l(V-E_l) \tag{2}$$

and the voltage-dependent ionic currents are expressed in the form:

$$I_i = \rho g_i a_i (V-E_i), \tag{3}$$

$$a_{i\infty} = 1/(1+\exp(s_i (V-V_{0i}))), \tag{4}$$

$$\dot{a}_i = \phi(a_{i\infty}-a_i)/\tau_i. \tag{5}$$

with i=*d*, *r*, *sd*, and *sr*. Here, E_i are the equilibrium potentials, g_i the maximum conductances at the reference temperature T_0, and a_i the voltage and time-dependent activation parameters. ρ allows for the temperature scaling of the ionic currents. V_{0i} and s_i are half-activation potentials and slopes, respectively, of the steady state activation curves.

Exceptions to the above formulations are the assumed instantaneous activation of the fast depolarizing current

$$a_d = a_{d\infty}, \tag{6}$$

and the direct coupling of the slow repolarizing current to the slow depolarizing current:

$$\dot{a} = \phi(\eta I_{sd} - k a_{sr})/\tau_{sr}. \tag{7}$$

Here, η denotes the coupling constant and k is a relaxation factor.

The temperature dependences are expressed in terms of the scaling parameters ρ and ϕ for the maximum conductances and the time constants, respectively:

$$\rho = 1.3^{(T-T_0)/\Delta}, \quad \phi = 3.0^{(T-T_0)/\Delta}. \tag{8}$$

Here, T is the temperature at which the receptor cells operate, T_0=25°C is the reference temperature, and Δ=10°C is a scaling temperature. Each time T increases by Δ, the maximum conductance increases by a factor 1.3 and the time constants by a factor 3.

To account for the effect of random dynamics we have applied Gaussian white noise according to the Fox-Mueller algorithm [19]:

$$g_w = (-4Dh\ln a)^{1/2}\cos 2\pi b \qquad (9)$$

with a and b being random numbers between 0 and 1; h denotes the integration step, and the noise intensity is adjusted by the dimensionless parameter D. The noise is directly added to the membrane potential.

With the above simple temperature scaling and with noise implemented in the model equations, the full variety of experimentally observed impulse pattern evolves almost naturally. Increasing the temperature speeds up the ionic kinetics and leads to a faster dynamics of the subthreshold oscillator. This is associated with a decrease in the number of spikes that can be triggered per oscillation cycle.

2.2. Role of noise in pattern formation. Fig. 1 reproduces some of the most characteristic patterns from experimental recordings for rat cold receptors [7] for direct comparison with the results of our modelling studies which are shown in the traces below. It can be seen that the model almost perfectly mimics all types of cold receptor discharges, but it also becomes evident that at least one type of pattern can be simulated only with the addition of noise. This is the pattern that consists of a mix of spike-generating and subthreshold oscillations (skippings) that typically occurs in the upper temperature range and can be seen in both experimental and modelling data (35°C, left diagrams) but not in the lowest diagram which is from a completely deterministic simulation (D=0). In this situation only the presence of noise allows the subthreshold oscillations to randomly exceed the threshold for spike-generation.

The second row shows the tonic firing patterns that typically can be seen in experimental recordings at normal skin temperatures around 30°C and which also occur in our simulations with the appropriate temperature scaling. Noise does not seem to have

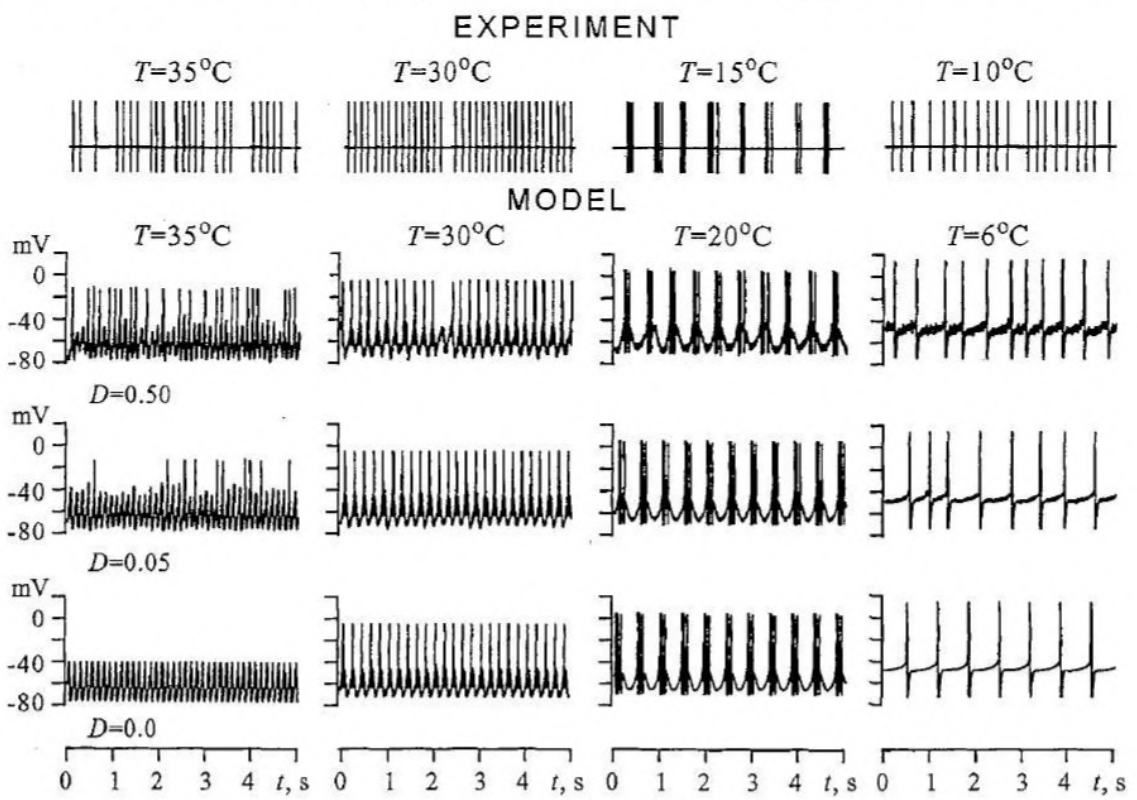

Fig. 1. Typical impulse patterns for cold receptors at different temperatures. Comparison of experimentally recorded spike trains (upper traces) and modelling results from deterministic simulations (D=0, lowest traces) and with addition of noise (D=0.05 and D=0.5, intermediate traces). The parameters of the numerical simulations are given in Ref. [20]

major influence on the pattern generation. There is a regular tonic discharge because each oscillation cycle succeeds to trigger a spike - with a single exception: at D=0.5 one of the oscillation cycles obviously fails to produce a spike. The upper trace indicates that a similar phenomenon may occur in the experimental recordings: a spike is missing within an otherwise regular tonic discharge. (Note that the simulation for D=0.5 and T=30°C has been shifted along the time axis for the missing spike to occur at the same time as the spike in the experimental sequence.) Although the missing spikes represent singular events, their occurrence suggests that noise cannot only induce spiking in otherwise completely subthreshold oscillations (as shown in the left traces) but can also prevent impulse generation in otherwise regularly spiking sequences. Such situations can cover a broad range of stimulus encodings.

In the third row of the figure we are comparing electrophysiological recordings and model simulations of different noise levels in the range of bursting discharges. More random input simply seems to induce more random fluctuations of spike-generation without any qualitative change of the pattern. This appears to also be the case at the lowest temperatures where the experimental recordings often exhibit irregular tonic discharges. The deterministic simulations generate completely regular discharges and the addition of noise is needed to produce the more realistically appearing irregular spike sequences.

With the addition of noise the model successfully reproduces the major types of experimentally recorded impulse patterns and it explains how these patterns can be related to the resonance behavior between slow subthreshold oscillations and spike generating mechanisms. The Huber/Braun is valuable not only because it successfully simulates stationary cold receptor discharges, but also as a generalized neuronal pattern generator of significant flexibility.

3. Transitions between β and γ rhythms

3.1. The Kopell model. In a neural system, the individual neuron is generally located in an excitatory or inhibitory network that provides a variety of inputs to the neuron, primarily via the synaptic currents. In the present section we consider a minimal model for a neural network capable of producing both β and γ oscillations. Developed by Kopell *et al.* [16], the model includes two excitatory pyramidal neurons and one inhibitory interneuron. The network architecture is illustrated in Fig. 2 where open and filled arrowheads represent excitatory and inhibitory connections, respectively. Solid lines indicate fixed connections, and dotted lines represent connections that are varied during the simulations. By contrast to the single neuron considered in Sec. 2, the interesting features of the present system are connected with the interaction of the different neurons. Many factors contribute to making the environment of the network noisy. All of these factors are regarded as random external fluctuations. As we have seen in the previous section it is likely that neurons can use such external fluctuations to process their input signals more

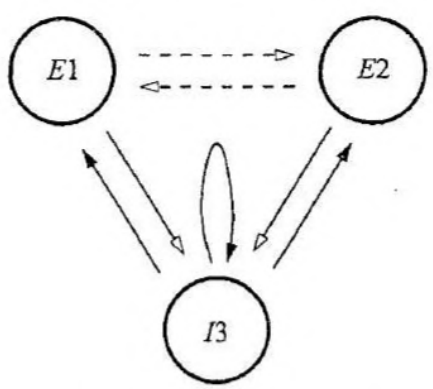

Fig. 2. Architecture of the Kopell oscillatory network. E1 and E2 are excitatory cells, and I3 is an inhibitory cell. Open and filled arrowheads represent excitatory and inhibitory connections, respectively. Solid lines indicate fixed connections, and dotted lines represent synapses whose efficacies are varied in the simulations

effectively. Here, we shall see how the presence of noise can generate transitions between different rhythmic modes in the network.

The Kopell model is based on Hodgkin-Huxley type neurons [21] which are modelled in accordance with the original formulation (rather than the simplified form used in the Huber/Braun model). There are no currents for subthreshold oscillations. Instead, there is an additional slow potassium current that accounts for after-hyperpolarization (ahp) in the excitatory neurons. The voltage of an excitatory neuron is controlled by the following differential equation:

$$c\dot{V} = -g_l(V-E_l) - g_{Na}m^3h(V-E_{Na}) - g_K n^4(V-E_K) \\ -g_{ahp}w(V-E_K) - i^e_{syn} + i^e_{appl}. \tag{10}$$

One recognizes the leak current $g_l(V-E_l)$, the sodium current $g_{Na}m^3h(V-E_{Na})$, the potassium current $g_K n^4(V-E_K)$, and the additional potassium current for after-hyperpolarization $g_{ahp}w(V-E_K)$. There is also a synaptic current input i^e_{syn} and a term for external current application i^e_{appl}. V is the membrane potential, E_j (j=Na or K) is the Nernst (or reversal) potentials for the respective ions, and g_j the corresponding conductances; c is the membrane capacitance.

The gating variables are assumed to obey the standard dynamical equations:

$$\dot{m} = \alpha_m(V)(1-m) - \beta_m(V)m, \tag{11}$$

$$\dot{h} = \alpha_h(V)(1-h) - \beta_h(V)h, \tag{12}$$

$$\dot{n} = \alpha_n(V)(1-n) - \beta_n(V)n, \tag{13}$$

$$\dot{w} = \alpha_w(V)(1-w) - \beta_w(V)w, \tag{14}$$

where the α and β - functions describe the voltage-dependent opening and closing rates for the various channels. For each excitatory neuron, a single equation controls the state of the synapses going from this neuron to others:

$$\dot{s}_e = \alpha_{s_e}(V)(1-s_e) - \beta_{s_e}s_e. \tag{15}$$

Synaptic input to an excitatory neuron (here, E1) results in a current

$$i_{syn,\mathrm{E1}}{}^e = g_{ee}s_{e,\mathrm{E2}}(V-E_e) + g_{ie}s_{i,\mathrm{I3}}(V-E_i). \tag{16}$$

In this expression, the s-variables refer to the presynaptic neurons (E2 and I3, respectively), whereas the voltage V refers to the postsynaptic neuron (E1). E_e and E_i denote the reversal potentials associated with excitatory and inhibitory synapses. A similar equation is used for the synaptic current of E2.

The inhibitory neuron I3 is very similar to E1 and E2, only the after-hyperpolarization-current is not included:

$$c\dot{V} = -g_l(V-E_l) - g_{Na}m^3h(V-E_{Na}) - g_K n^4(V-E_K) - i^i_{syn} + i^e_{appl}. \tag{17}$$

Noting that w does not appear, the remaining gating variables for the inhibitory neuron I3 are controlled by Eqs (11-13).

Inhibitory synapses are governed by the equation:

$$\dot{s}_i = \alpha_{s_i}(V)(1-s_i) - \beta_{s_i}s_i. \tag{18}$$

The inhibitory neuron receives inputs from E1 and E2 as well as from a mechanism of self-inhibition:

$$i^{i}_{syn,I3} = (g_{ei}s_{e,E1}+g_{ei}s_{e,E2})(V-E_e) + g_{ii}\,s_{i,I3}(V-E_i). \quad (19)$$

The detailed description of the various functions and parameter values can be found in the original paper [16]. Two parameters are varied in the present study: g_{ee}, the strength of the connections between E1 and E2, and g_{ahp}, the maximal conductance for the slow potassium ion channels.

The Kopell model demonstrates three main network modes.

• For low values of the two parameters, the three neurons spike in synchrony with a frequency in the γ band;

• If g_{ahp} is increased, the E1 and E2 neurons start to miss every other spike, lowering their individual frequencies into the β band. However, since E1 and E2 are out of phase, the population of excitatory neurons as a whole continues to produce γ oscillations;

• Increasing the connection strengths between E1 and E2 makes the excitatory neurons spike simultaneously, thereby producing β oscillations.

The results of scanning over a two-dimensional parameter space are shown in Fig. 3. Here, one can distinguish four to five different oscillatory modes. For low values of g_{ahp}, the region denoted γ corresponds to parameter values that generate γ rhythms where all neurons (E1, E2, and I3) spike in every cycle. The «γ population» state γ_{pop} is located to the left with intermediate values of g_{ahp}. In this region, the neurons E1 and E2 both demonstrate β rhythms of 16-17 Hz, but their overall behavior is found to produce oscillations in the γ band. There is a large region β occupied by β oscillations where E1 and E2 are in full synchrony with half the frequency of the γ rhythm. With decreasing g_{ahp}, they evolve into the β population β_{pop}. This state produces a β rhythm, but only half as powerful as the β state described earlier since only one excitatory neuron (E1) spikes. Within a range of parameters one can observe high-order solutions with different combinations of spiking and silent states in the two excitatory neurons [22]. The dynamics seems to be limited in the g_{ahp} direction by the appearance of a silent-state, in which E1 and E2 never spike due to the effects of the after-hyperpolarization current in combination with the spontaneous spiking of the I3 neuron. In the gray region, the γ_{pop} and the β modes coexist. The observation of a large region with coexisting solutions may have important inferences with respect to brain function. The question is: Can the Kopell model switch between the coexisting states? Physiologically, the externally applied current i^{e}_{appl}, together with ionic and synaptic currents, could represent the influence of other neurons of the brain. As previously noted, this influence may be considered in many instances as stochastic. Let us, therefore, examine the influence of fluctuations on the switching process.

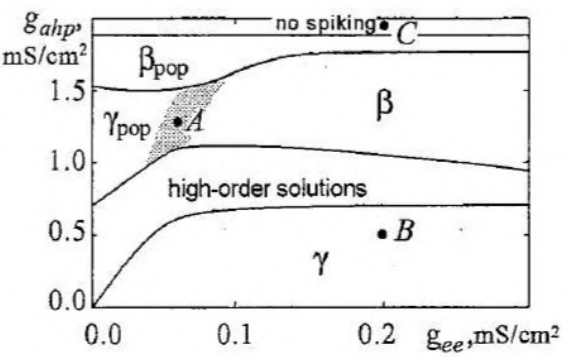

Fig. 3. Different oscillatory modes as functions of g_{ee} (the coupling between excitatory neurons) and g_{ahp} (the conductance for the slow K-channel in excitatory neurons). In the gray region the γ_{pop} and β modes coexist. In the region denoted high-order solutions we find a great variety of frequency-locked states

3.2. Stochastic dynamics. Since noise may have different origins and can contribute in different ways, we assume that our network operate in a noisy field (Fig. 2). We represent this as Gaussian noise $\xi(t)$ with intensity D added to the first equations of each neuron.

Switchings between coexisting γ_{pop} *and* β *modes.* With noise of sufficient intensity, the system switches between two states. This can be characterized in different ways. First, we can introduce a phase shift between the spiking events in E1 and E2 as $\Delta\phi=2\pi t/T$. In this case, the system can be considered as bistable where a trajectory alternates between $\Delta\phi=0$ and $\Delta\phi=\pi$. With increasing noise intensity, hopping becomes more frequent. Secondly, the system can be described via the overall dynamics of the excitatory neurons. Let us choose the parameters to be in the region where γ_{pop} and β oscillations coexist (point *A* in Fig. 3). In the noiseless case, with the applied initial conditions, the resulting output oscillations is a β rhythm. This corresponds to a sharp peak at f_β=17 Hz. With noise, an additional peak appears at f_γ=34 Hz. With increasing noise, the peak at f_β becomes broader and smaller in amplitude.

To describe the switching dynamics we can evaluate different characteristics. Fig. 4, *a* illustrates the behavior of the residence time (solid and dotted curves) in the bistable system with $\Delta\phi=0$ and $\Delta\phi=\pi$. With vanishing noise, the system remains in the $\Delta\phi=0$ state and the residence time tends to infinity. When noise is introduced, the system can switch to the other state. With increasing noise, the residence times in the two states tend to become equal.

A quantitative measure of coherence is the so-called regularity coefficient which can be calculated as [14]:

$$R = \langle\tau\rangle/(\langle\tau^2\rangle-\langle\tau\rangle^2)^{1/2}, \qquad (20)$$

where τ is specified as the switching time between the states (Fig. 4, *a*, dashed curve) or as the interspike interval (Fig. 4, *b*). The time averaged duration identifies the mean period and, hence, the mean frequency $\langle f\rangle=1/\langle\tau\rangle$ of the noise-activated oscillations. Figure 4, *a* illustrates how the coherence of the switching events (dashed curve) grows monotonically when the noise intensity is increased. Very strong noise causes fast switching. The residence time then becomes less than two interspike periods, and our two-state approach no longer applies. The spike train provides an efficient way to code a sequence of action potentials with nearly the same shape since the most important information in neuronal systems is widely believed to be coded in the time sequence of action potential generation [23]. The spike train is a binary time series with a value 1 at the time of action potential generations and 0 at other times. We analyzed the coherence properties for spike trains in the presence of noise. The results of a calculation of the regularity coefficient (20) as a function of noise intensity are shown in Fig. 4, *b*. The curve is seen to display a maximum for noise intensities around D=0.4. For weak noise, the contribution of γ_{pop} to the whole spike train is small. At the optimal noise intensity β and γ_{pop} contribute equally to the spiking train. Strong noise destroys the β rhythm, and the regularity decreases. This represents an example of coherence resonance in the noise-induced switching between different modes of the neural system.

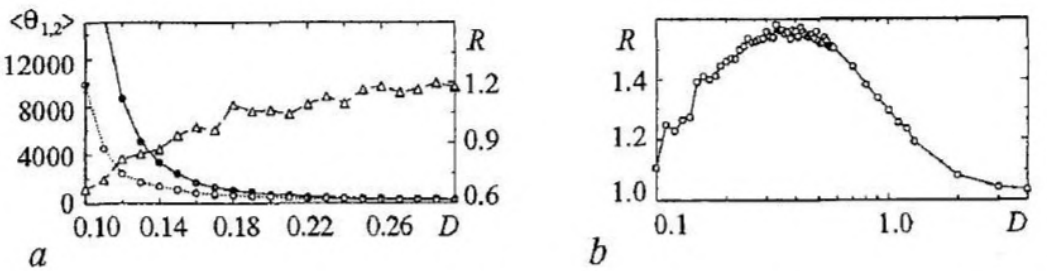

Fig. 4. (*a*) Residence time $\langle\theta_{1,2}\rangle$ for $\Delta\phi=0$ (solid curve) and $\Delta\phi=\pi$ (dotted curve) and regularity coefficient R of the switching time (dashed curve) as functions of the noise amplitude; (*b*) regularity coefficient R calculated from the interspike intervals; g_{alip}=1.25 mS/cm^2, g_{ee}=0.05 mS/cm^2. $\Delta\phi$ represents the phase shift between the spiking events in the excitatory neurons E1 and E2

Hopping between γ and β regimes. In the diagram presented in Fig. 3, regions of γ and β rhythms are separated by the region of high-periodic solutions. Fixing the parameters at the point B of the diagram, when adding noise we observe a *direct* transition between the main rhythms. The residence time in the β regime now grows with increasing noise intensity. Our measure of coherence calculated over the interspike intervals indicates a well-pronounced maximum at some optimal noise intensity at which β and γ spike trains alternate in a regular way (Fig. 5). Here, we observe another example of regularized hopping events induced by applied noise, but now with one of the involved states being unstable for the considered parameters.

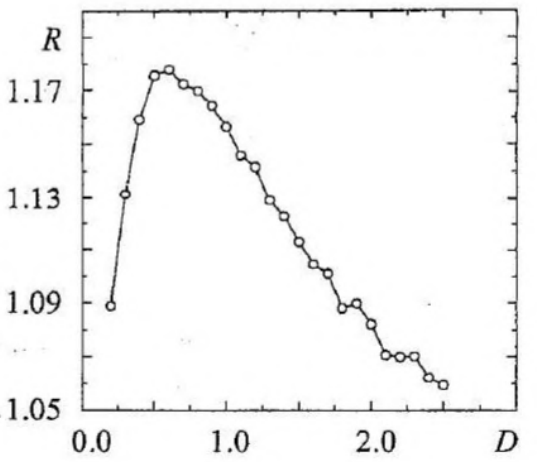

Fig. 5. Coherence dynamics of interspike intervals in the Kopell model for g_{ahp}=0.5 mS/cm^2 and g_{ee}= =0.2 mS/cm^2. As before, D represents the noise amplitude

Onset of spiking dynamics. Let us hereafter see how noise can cause firing events in this local network. (Parameter values corresponding to point C in Fig. 3.) It is known that the behavior of spike trains can exhibit coherence resonance at an optimal noise intensity, as described for a single Hodgkin-Huxley model by Lee *et al.* [24]. In this case, noise affects the dynamics of the system in two ways: (i) increasing the noise intensity decreases the silence (activation) time so that the contribution of the spiking dynamics increases. This enhances the regularization of spiking dynamics of the membrane potential. (ii) noise also produces amplitude and phase fluctuations of the firing dynamics, destroying the periodicity in spiking events. The competition of these two mechanisms produces the phenomenon of coherence resonance, i.e. a maximal degree of coherence for an optimal noise level. This phenomenon is responsible for the first peak of coherence for E1 (Fig. 6). With vanishing connection between the excitatory cells (g_{ee}=0.0), E2 demonstrates coherence of spiking events at a higher noise intensity because of its different internal parameters. Due to inhibitory synapses (controlled directly in the Kopell model by varying g_{ii} and g_{ie}), the first neuron adjusts its spiking train and demonstrates a secondary coherence resonance at higher noise intensity (Fig.6, *a*).

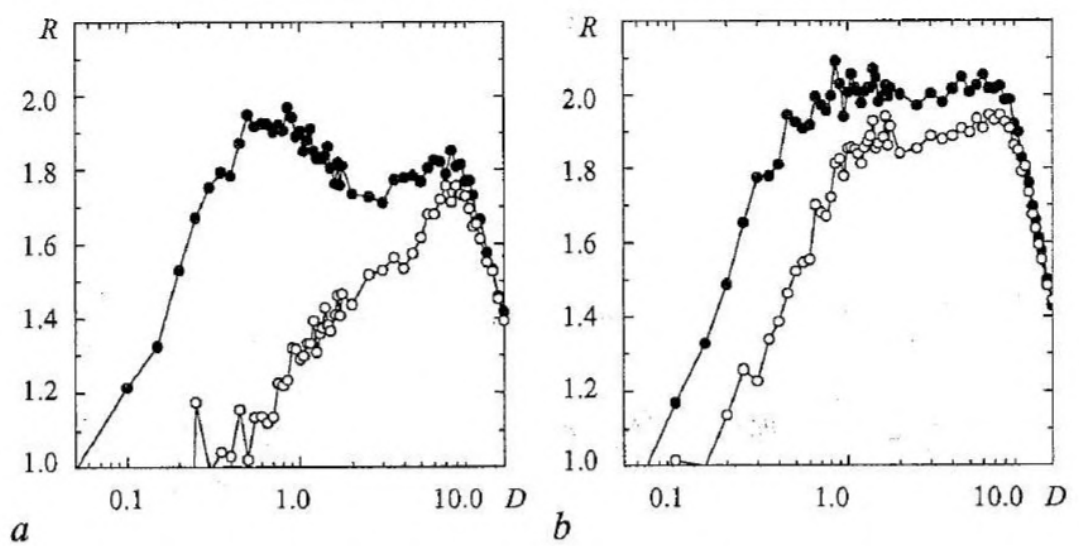

Fig. 6. Regularity for (*a*) g_{ahp}=2.0 mS/cm^2, g_{ee}=0.0 mS/cm^2 and (*b*) g_{ahp}=2.0 mS/cm^2, g_{ee}=0.2 mS/cm^2. Note, how the two peaks observed in (*a*) are closer to one another in (*b*)

When the E1-E2 connection is introduced (g_{ee}=0.2 mS/cm^2), the two peaks approach one another and the excitable units demonstrate a well-pronounced peak of coherence at the same noise intensity. This is illustrated in Fig. 6, *b*. Because of the synchronization effects, the maximal value of R is higher than in the previous case [25].

4. Noise-induced rhythms

Let us hereafter focus on *noise-induced* rather than on noise-activated oscillatory modes. This implies that we focus on time scales that are generated and controlled by noise and do not exist in the deterministic case. We provide experimental observation of such multimode behavior and investigate the conditions of generation and entrainment of the specified modes.

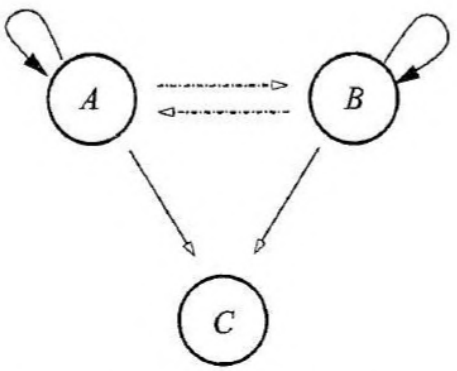

Fig. 7. Schematic presentation of a breathing rhythm generator for a snail

The purpose of this section is to describe the two-mode stochastic behavior of an electronic system that has been constructed as a hard-wired version of the simplest breathing rhythm generator for a snail (Fig. 7) [26]. A single monovibrator circuit [27], being the functional unit in our electronic experiment, captures the essential aspects of excitable systems generating a single electric impulse whenever the input voltage exceeds the threshold level. The implementation of interacting excitable units shown in Fig. 8, *a* contains self- and mutually inhibitory coupling chains that can increase the threshold voltages of the first (V_{th1}) and second (V_{th2}) units. Each coupling chain contains a rectifier and a low-pass filter with coupling strength g_{ij} and time constant τ_{ij}, where i, j denote the unit numbers. Note that the self-inhibitory time constants were chosen to be equal and to be greater than the mutually inhibitory time constants, i.e., $\tau_{11}=\tau_{22}>\tau_{12}=\tau_{21}$.

With a small noise intensity D (which is the same for the two units), both excitable units keep silent most of the time, and their threshold voltages remain equal ($V_{th1}\approx V_{th2}$). For intermediate noise levels, the coupling influence on the threshold voltages becomes

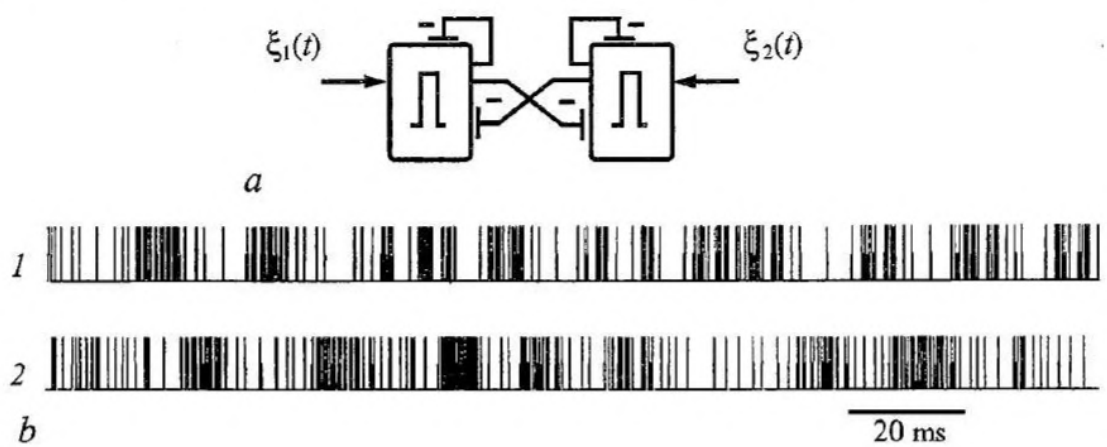

Fig. 8. (*a*) Two monovibrators with delayed inhibitory couplings imitate the simple neural circuit. (*b*) Stochastic spike trains generated by the first and second excitable units. Antiphase behavior is indicated on the average

significant. At the same time, since mutual inhibition makes the in-phase regime unstable, one of the two units gets the upper hand with respect to its ability to suppress the firings of the other. However, with intensive firing, the slow self-inhibitory chain with rate τ_{11} (or τ_{22}) comes into operation and suppresses the activity of the stronger unit. This creates better conditions for excitation of the other unit, and the process continues in an alternating manner, producing a behavior with time-varying firing rates for the two excitable units (Fig. 8, *b*).

In this operating regime, two peaks in the power spectrum are clearly distinguished (Fig. 9, *a*). The high frequency peak corresponds to noise-induced oscillations in the single system while the low frequency peak reveals a new noise-induced oscillatory mode. Hence, the system of coupled excitable units generates a new oscillatory mode that is characterized by the values of τ_{ij} and by the relation between the noise intensity and the initial threshold voltages (V_{th1},V_{th2}). Fig. 9, *b* demonstrates how the frequencies of these oscillations (open circles) depend on the noise intensity. Inspection of the figure clearly shows that with increasing noise strength, both frequencies grow (i.e., they are noise-controlled), but the growth rates are different (i.e., they operate independently of each other). For strong noise, an excitable system can be immediately pushed out from the equilibrium state in spite of the threshold voltage. The low frequency peak in the power spectrum disappears, and the additional time scale no longer exists.

The regularity of the low-frequency stochastic oscillations is related to the process of pulse generation in the state of each excitable unit. Hence it is determined by the effect of coherence resonance [27]. Fig. 9, *b* illustrates how the output regularity R (filled circles) is suddenly increased when low frequency oscillations appear, but the peak at the noise-induced eigenfrequency f_2 becomes washed out because of the threshold modulation.

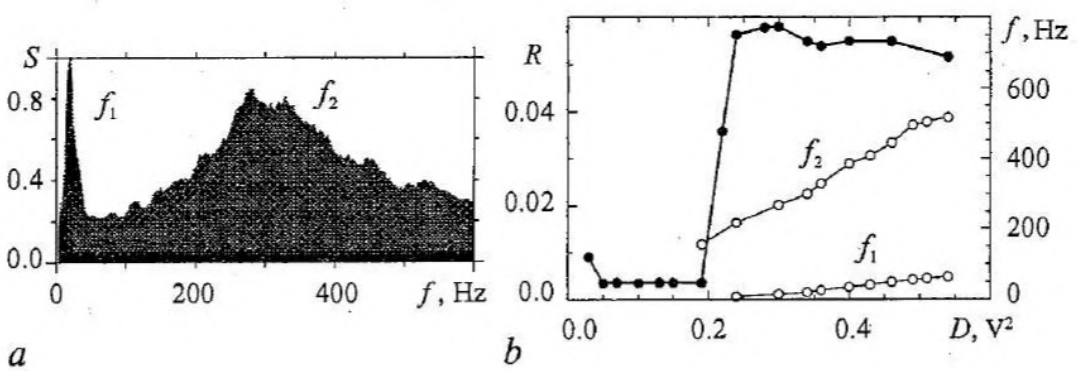

Fig. 9. Two-mode dynamics in the excitable system presented in Fig. 8*a*. (*a*) Power spectrum with well-pronounced peaks (D=0.34V^2) and (*b*) peak frequencies (open circles) and measure of regularity R (filled circles) *vs* noise intensity D

5. Discussion

We considered noise-activated and noise-induced rhythms in models representing three different neural systems: (i) a single-neuron model of a peripheral pattern generator (a mammalian cold receptor); (ii) a small neural network (the Kopell model) that can account for the coexistence of β and γ rhythms in the brain, and (iii) a coupled monovibrator system that can serve as a model of a simple breathing rhythm generator. Our results indicate that the interaction between stochastic phenomena and complex deterministic dynamics may lead to a variety of different phenomena of importance for neural rhythm generation.

The single neuron model mimics the discharge pattern of peripheral cold receptors where impulse generation is determined by slow-wave oscillations which trigger one or

more impulses during their depolarizing phases. This holds true for both deterministic and stochastic simulations with the exception that noise can induce spiking as well as skipping around the onset of period-one activity. In the regular bursting range noise does not produce any qualitative effects on the pattern but mainly smoothens the deterministically abrupt transitions. In the chaotic regime noise destroys the fine structure of the bifurcations. Thus, noise is assumed to play as essential role in sensory neurons: spike generation is clearly phase-locked to the underlying oscillations but noise determines the threshold crossings and hence the times at which spikes are generated. In addition to serving as cellular substates for synchronization in neuronal networks, subthreshold oscillations can also serve as cellular substates for a sensitive and differential neuromodulatory control based on the intrinsic oscillatory dynamics as optimized by naturally occurring noise sources. Further studies on subthreshold oscillating neurons should encompass the interesting neuromodulatory and encoding properties which arise from cooperative effects of oscillations with noise.

The neuronal network model also displays spiking patterns that are modified in an essential manner by the presence of noise. Especially in the area with coexisting solutions, noise causes the network to jump from one state to the other. There is a sharp transition between the oscillatory mode and a hopping state between the coexisting solutions, and this transition is controlled by the noise intensity. The output signal demonstrates quite «regular» switchings for a certain noise intensity. Moreover, noise can initiate switchings in the region where the main β and γ oscillations are separated by high-periodic solutions in the parameter space. In this case, we again observe an optimal noise intensity at which the jumping behavior becomes coherent. A particularly interesting finding is that, due to synaptic inhibitory interaction, the excitatory cells can demonstrate double coherence resonance [28]. With the introduction of a coupling between these neurons, the two peaks of regularity merge together, giving rise to further gain of regularity by virtue of synchronization.

We also showed that a simple system of coupled excitable functional units can generate a few oscillatory modes that are induced and controlled by noise [29]. Possible advantages of multimode dynamics may include: (i) increased sensitivity via coherence resonance; we have found multiple coherence resonance phenomenon related to different frequency entrainments and to the appearance of additional time scales; (ii) expanded flexibility. The presence and interaction of two distinct oscillatory modes enrich the dynamical patterns. The electronic approach involving excitable stochastic units with self- and mutually inhibitory couplings can be applied to simulate neuron systems with a priory given phase relations.

This work was partly supported by INTAS grant 01-2061 and RFBR grant 01-02-16709. O.S. acknowledges INTAS (Grant YSF 01/1-0023) and the Lundbeck Foundation.

References

1. *Anishchenko V.S.* Dynamical Chaos: Models and Experiments. World Scientific, Singapore, 1995.

2. *Anishchenko V.S., Astakhov V.V., Neiman A.B., Vadivasova T.E., and Schimansky-Geier L.* Nonlinear Dynamics of Chaotic and Stochastic Systems. Springer Verlag, Berlin, 2002.

3. *Eckhorn R., Bauer R., Jordan W., Brosch M., Kruse W., Munk W., and Reitboeck H.J.* Coherent oscillations: A mechanism of feature linking in the visual cortex? Biol. Cybern. 60 (1988), 121-130.

4. *Gray C.M., König P., Engel A.K., and Singer W.* Oscillatory responses in cat

visual cortex exhibit inter-columnar synchronization which reflects global stimulus properties, Nature 338 (1989), 334-337.

5. *Braun H.A., Bade H., and Hensel H.* Static and dynamic discharge patterns of bursting cold fibers related to hypothetical receptor mechanisms. Pflügers Arch. 386 (1980), 1-9.

6. *Braun H.A., Schäfer K., Wissing H., and Hensel H.* Periodic transduction processes in thermosensitive receptors // Sensory Receptor Mechanisms (eds W. Hamann, A. Iggo), World Scientific, Singapore, (1984), 147-156.

7. *Braun H.A., Huber M.T., Dewald M., Schäfer K., and Voigt K.* Computer simulations of neuronal signal transduction: The role of nonlinear dynamics and noise // Int. J. Bifurcation &. Chaos.1998. Vol. 8. Pp. 881-889.

8. *Braun W., Eckhardt B., Braun H.A., and Huber M.T.* Phase space structure of a thermoreceptor // Phys. Rev. E. 2000. Vol. 62. Pp. 6352-6360.

9. *Feudel U., Neiman A., Pei X., Wojtenek W., Braun H.A., and Huber M.T.* Homoclinic bifurcations in a Hodgkin-Huxley model of thermally sensitive neurons // Chaos. 2000. Vol. 10. Pp. 231-239.

10. *Tuckwell H.C.* Stochastic Processes in the Neurosciences. SIAM, Philadelphia, 1989; Taylor J.G., Neurodynamics, (eds F. Faseman and H.D. Doebner), World Scientific, Singapore (1991), 129-164.

11. *Braun H.A., Wissing H., Schäfer K., and Hirsch M.C.* Oscillation and noise determine signal transduction in shark multimodal sensory cells // Nature. 1994. Vol. 367. Pp. 270-273.

12. *Russell D.F., Wilkens L.A., and Moss F.* Use of behavioural stochastic resonance by paddle fish for feeding // Nature. 1999. Vol. 402. Pp. 291-294.

13. *Nakamura K.* Stochastic Resonance in the FitzHugh-Nagumo Neuron Model // Proc. Inst. Natural Sci. 2000. Vol. 35. Pp. 179-185.

14. *Pikovsky A.S. and Kurth J.* Coherence resonance in a noise-driven excitable system // Phys. Rev. Lett. 1997. Vol. 78. Pp. 775-778.

15. *Neiman A., Pei X., Russell D., Wojtenek W., Wilkens L., Moss F., Braun H.A., Huber M.T., and Voigt K.* Synchronization of the noise electrosensitive cells in the paddlefish // Phys. Rev. Lett. 1999. Vol. 82. Pp. 660-663.

16. *Kopell N., Ermentrout G.B., Whittington M.A., and Traub R.D.* Gamma rhythms and beta rhythms have different synchronization properties // Proc. Nat. Acad. Sci. USA. 2000. Vol. 97. Pp. 1867-1872.

17. *Bressler S.L., Coppola R., and Nakamura R.* Episodic multiregional cortical coherence at multiple frequencies during visual task performance // Nature. 1993. Vol. 366. Pp. 153-156.

18. *Braun H.A., Huber M.T., Anthes N., Voigt K., Neiman A., Pei X., and Moss F.* Interaction between slow and fast conductances in the Huber/Braun model of cold-receptor discharges // Neurocomputing. 2000. Vol. 32-33. Pp. 51-59.

19. *Fox R.F., Gatland I.R., Roy R., and Vemuri G.* Fast accurate algorithm for numerical simulation of exponentially correlated colored noise // Phys. Rev. A. 1988. Vol. 38. Pp. 5938-5940.

20. 1) Equilibrium potentials: $E_{sd}=E_d=50$, $V_{sr}=V_r=-90$, $V_l=-60$ (mV); 2) ionic conductances: $g_l=0.1$, $g_d=1.5$, $g_r=2.0$, $g_{sd}=0.25$, $g_{sr}=0.4$ (mS/cm^2); 3) membrane capacitance: $C=1$ (μF/cm^2) gives a passive time constant $\tau_M=C/g_l=10$ (ms); 4) activation time constants: $\tau_r=2$, $\tau_{sd}=2$, $\tau_{sr}=2$ (ms); 5) slope of steady state activation: $s_d=s_r=0.25$, $s_{sd}=0.09$; 6) half activation potentials: $V_{0d}=V_{0r}=-25$, $V_{0ds}=-40$ (mV); 7) coupling and relaxation constants for I_{sr}: $\eta=0.012$, $k=0.17$; 8) reference temperature: $T_0=25°(C)$.

21. *Hodgkin A.L. and Huxley A.F.* A quantitative description of membrane current and its application to conduction and excitation in nerve // J. Physiol. 1952. Vol. 117. Pp. 500-544.

22. *Fausboll A.* Analysis of a Minimal Network of Cortical Neurons. MSc. Thesis, DTU, Denmark, 2001.

23. *Moore G.P., Perkel D.H., and Segundo J.P.* Statistical analysis and functional interpretation of neuronal spike data // Ann. Rev. Physiol. 1966. Vol. 28. Pp. 493-522.

24. *Lee S.-G., Neiman A., and Kim S.* Coherence resonance in a Hodgkin -Huxley neuron // Phys. Rev. E. 1998. Vol. 57. Pp. 3292-3297.

25. *Postnov D.E., Setsinsky D.V., and Sosnovtseva O.V.* Stochastic synchronization and the growth in regularity of the noise-induced oscillations // Tech. Phys. Lett. 2001. Vol. 27. Pp. 49-55.

26. *Rosenzweig M.R., Leiman A.L., Breedlove S.M.* Biological Psychology. Sinaur Associated, Inc. Sunderland, Massachusetts, 1996.

27. *Postnov D.E., Han S.K., Yim T., and Sosnovtseva O.V.* Experimental observation of coherence resonance in cascaded excitable systems // Phys. Rev. E. 1999. Vol. 59. 3791-3794; Han S.K., Yim T., Postnov D.E., and Sosnovtseva O.V. Interacting coherence resonance oscillators // Phys. Rev. Lett. 1999. Vol. 83. Pp. 1771-1774.

28. *Sosnovtseva O.V., Setsinsky D., Fausboll A., Mosekilde E.* Transitions between beta and gamma rhythms in neural systems // Phys. Rev. E. 2002. Vol. 66. 041901(6).

29. *Postnov D.E., Sosnovtseva O.V., Han S.K., and Kim W.S.* Noise-induced multimode behavior in excitable systems // Phys. Rev. E. 2002. Vol. 66. 016203(5).

Department of Physics, The Technical University of Denmark,
Physics Department, Saratov State University, Russia
Institute of Physiology, University of Marburg, Germany

Received 31.07.03

УДК 532.517, 517.9, 621.373

НЕЙРОННЫЕ ГЕНЕРАТОРЫ РИТМА В ПРИСУТСТВИИ ШУМА

E. Mosekilde, О.В. Сосновцева, Д.Э. Постнов, H.A. Braun, M.T. Huber

Исследуются динамические особенности генерации последовательности спайков в присутствии шума для трех различных моделей нейронных генераторов ритма: простой нейронной модели, которая воспроизводит импульсную модуляцию для кодирования температуры в холодовых рецепторах млекопитающих, минимальной нейронной сети, описывающей переходы между бета- и гамма-ритмами в мозге, и электронного переключательного устройства, представляющего собой простой генератор дыхательного ритма улитки. Мы показываем, что шум может объяснить множество особенностей в наблюдаемой последовательности спайков, вызывать когерентные переключения между различными состояниями, и индуцировать новые ритмы в малых нейронных ансамблях.

Erik Mosekilde received the M.Sc. in electrical engineering from the Technical University of Denmark (DTU) in 1966, the Ph.D. in solid state physics from DTU in 1968, and the Dr.Sc. in semiconductor instabilities from the University of Copenhagen in 1977. In 1970 he was a postdoctoral fellow at IBM Watson Research Center in Yorktown Heights, New York. He has been a visiting scientist at a number of different universities in Europe and North America. He is a co-author of 190 scientific papers and of several books, including two recent books on «Topics in Nonlinear Dynamics» and «Chaotic Synchronization». His main interests are modeling of complex systems and applications of nonlinear dynamics. He is a Professor in nonlinear dynamics and a Head of the Department of Physics at DTU, Denmark.

Olga Sosnovtseva received the M.Sc. from Saratov State University, Russia in 1989, and the Ph.D. degree in Physics and Mathematics in 1996, also from Saratov State University. Since 2001 she has been a postodoctoral fellow at The Technical University of Denmark. She is co-author of 40 scientific papers. Her current interests are within the field of nonlinear dynamics and modelling of biological systems. E-mail: olga@fysik.dtu.dk

Dmitry Postnov is a professor of the Chair of Radiophysics and Nonlinear Dynamics of Saratov State University, Candidate of Science in Physics and Mathematics since 1990, Doctor of Science in Physics and Mathematics since 2001. He is an author of 56 papers in scientific journals and of book «Chaotic Synchronization. Applications to living systems» (World Scientific, 2002).
E-mail: postnov@chaos.cas.ssu.runnet.ru

Hans Albert Braun is head of the Neurodynamics Group at the Institute of Physiology at the University of Marburg in Germany. He has been trained as electronic engineer at the Technical University in Karlsruhe where he obtained a degree in «Electrobiology». In course of a supplementary study of «Human Biology» he obtained his PhD at the Medical Faculty of the University of Marburg.

His research involves experiments and models of neuronal encoding and neuromodulatory processes in peripheral sensory receptors (thermo- and electroreceptors) and hypothalamic neurones (neuroendocrine functions) including computer modelling studies of affective disorders. The aim is the understanding of neuronal systems dynamics at different levels and to elucidate their functional principles.

Hans A. Braun is member of several scientific societies and has been honored with the fellowship of the Biophysics Division of the American Physical Society. E-mail: braun@mailer.uni-marburg.de

Martin Tobias Huber is university lecturer of biological psychiatry and neuroinformatics at the Department of Psychiatry and Psychotherapy of the University of Marburg. His research interests include clinical and modelling studies of disease-relevant features of short- and longtterm changes in biological systems such as neuromodulation, sensitivity adjustment, sensitization and adaptation. The aim of these studies is the characterization of normal and pathological systems biology with particular emphasis on the biological psychiatry of affective disorders and schizophrenia.